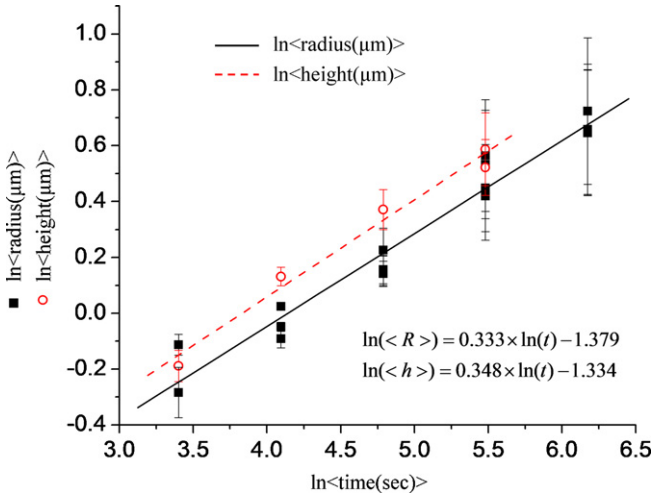

Fig. 4. Data plot of average radius vs time and height vs time Cu_6Sn_5 in reaction between 55Sn45Pb and copper at 200 °C.

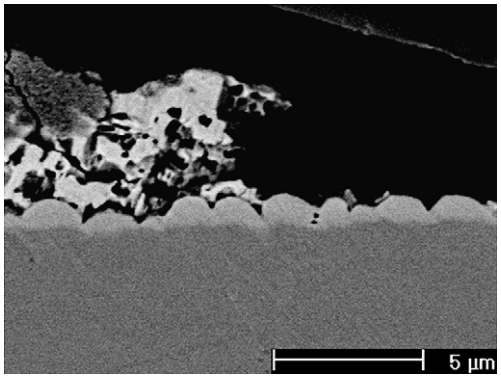

Fig. 5. Cross-sectional SEM image of Cu_6Sn_5 formed by reaction between 55Sn45Pb solder and copper at 200 °C for 30 s.

with the theoretical curve. Even though there was a small deviation, the experimental data showed fairly good agreement with the FDR model. The equation for the theoretical normalized curve of size distribution shown in Fig. 6a is given as [4]

$$g(u) = c\frac{u}{(2-u)^4}\exp\left(-\frac{4}{2-u}\right)$$

where u is the scaled particle size, defined as $u = r/\langle r\rangle$, and $g(u)$ is the probability density.

$$c = \left(\int_0^2 \frac{x}{(2-x)^4}\exp\left(-\frac{4}{2-x}\right)\mathrm{d}x\right)^{-1} = 0.0169$$

so that $g(u)$ is normalized to

$$\int_0^2 g(u)\mathrm{d}u = 1$$

The theoretical value of the standard deviation is

$$\sigma = \sqrt{\int_0^2 (u-1)^2 g(u)\mathrm{d}u} = 0.331$$

The theoretical value of skewness is

$$\frac{1}{\sigma^3}\int_0^2 (u-1)^3 g(u)\mathrm{d}u = -0.433$$

and the kurtosis is

$$\frac{1}{\sigma^4}\int_0^2 (u-1)^4 g(u)\mathrm{d}u - 3 = -0.403$$

Table 2 presents values of standard deviation, skewness and kurtosis, measured after different reflow times. Their average values were 0.423, −0.133 and −0.670, respectively.

Because cross-sectional SEM images were used to measure the height of the scallops, the number of scallops measured is much less than in the case of the radius distribution where the radius of scallops was measured from top-view images. Therefore, the height measurement data shown here is not statistically as reliable as the radius measurement, although the growth exponent of height vs time was also close to 1/3. The aspect ratio between height and radius remained almost constant. The average value of aspect ratio was 1.05.

4. Discussion

On the FDR model, the major differences from the LSW model are the constant surface area of growth and the existence of channels between scallops. The width of channel has not been measured directly, so the calculation based on experimental measurement is very important to the model. The constant k in Eq. (2) is composed of several thermodynamic parameters. To make a rough estimation of the channel width, one can take $C_i \approx 6/11$, $n/n_i \approx 1$, $D \approx 10^{-5}$ cm^2 s^{-1} and $C^b - C^e \approx 0.001$. $C^b - C^e$ was estimated by numerical thermodynamic calculation [4]. As $k = 2.10 \times 10^{-14}$ cm^3 s^{-1}, the channel width is calculated to be $\delta = 2.54$ nm, which means the channel width is in the nanometer scale. To validate the calculated channel width roughly, one can consider the upper and lower bounds of the channel width. The lower bound of the channel width is 0.5 nm, which is a typical grain boundary width in the solid state. If one takes a diffusivity of 10^{-8} cm^2 s^{-1}, which is on the order of the diffusivity of all fcc metals at their melting point, it should be the highest grain boundary diffusivity in the solid state, and the calculated channel width will represent an upper bound. Fig. 7 is a plot of diffusivity vs channel width. If one assumes a diffusivity of 10^{-8} cm^2 s^{-1}, the channel width is 2.54 μm. Obviously, this is an unreasonably large value because this value is comparable with the average diameter of the scallops. If one takes the channel width as 0.5 nm, the diffusivity is 5×10^{-5} cm^2 s^{-1}. Again, this is a high diffusivity for liquid, not for grain boundary. However, the calculated channel width needs to be confirmed experimentally. Wetting a molten SnPb solder on a bulk Cu_6Sn_5 surface will provide deep penetration of the

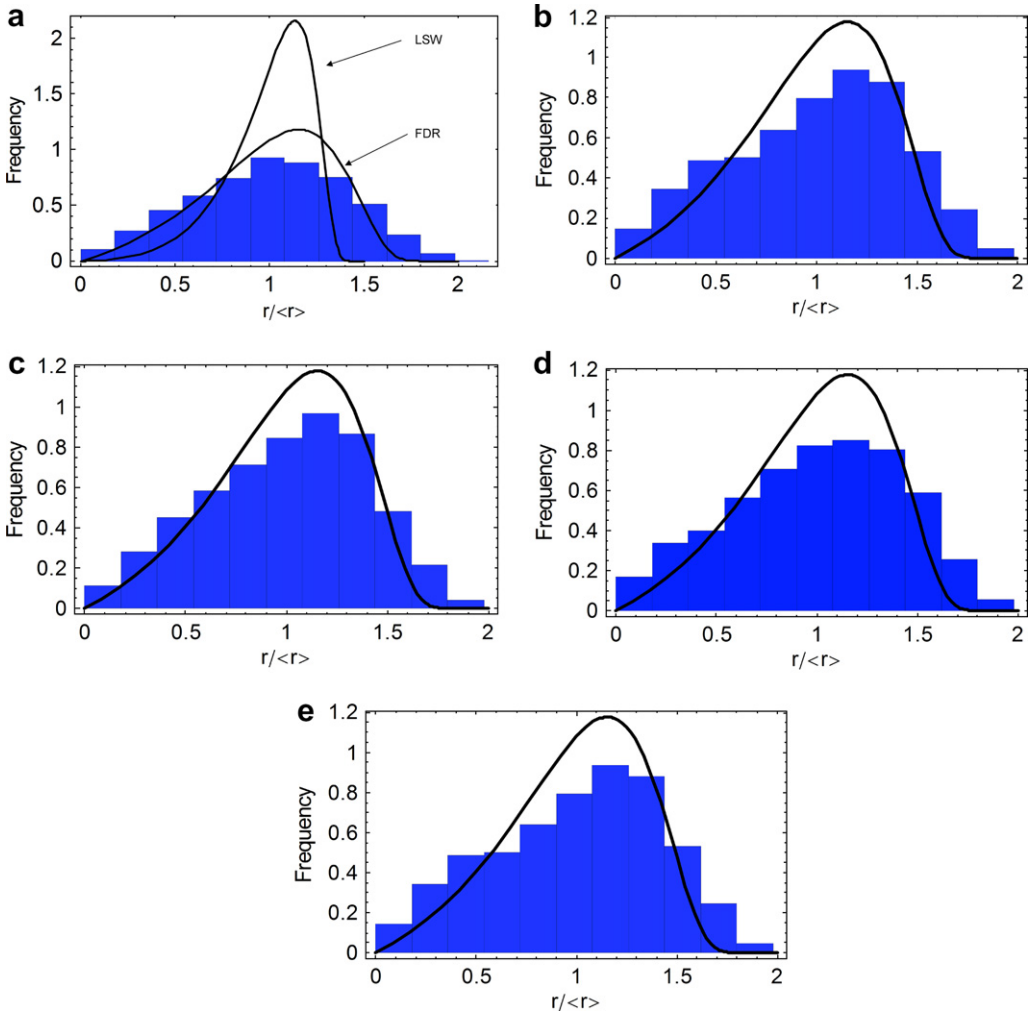

Fig. 6. Normalized PSD Cu_6Sn_5 scallops of (a) 30 s, (b) 1 min, (c) 2 min, (d) 4 min and (e) 8 min reflow. In (a), theoretical curves from LSW theory and FDR theory are shown for comparison.

Table 2
Statistical parameters of PSD of Cu_6Sn_5 in reaction between 55Sn45Pb and copper at 200 °C

Time (s)	Average radius $\langle r \rangle$ (μm)	Standard deviation σ, of $r/\langle r \rangle$	Skewness of $r/\langle r \rangle$	Kurtosis of $r/\langle r \rangle$
30	0.753	0.408	−0.126	−0.642
30	0.894	0.425	−0.096	−0.654
60	0.913	0.441	0.113	−0.575
60	1.025	0.415	−0.183	−0.628
60	0.953	0.406	−0.143	−0.662
120	1.164	0.428	−0.082	−0.560
120	1.169	0.410	−0.142	−0.572
120	1.253	0.434	−0.033	−0.743
120	1.152	0.399	−0.215	−0.618
240	1.566	0.455	−0.141	−0.796
240	1.760	0.433	−0.074	−0.712
240	1.522	0.417	−0.200	−0.667
240	1.704	0.419	−0.222	−0.718
480	1.933	0.428	−0.233	−0.740
480	1.908	0.417	−0.101	−0.630
480	1.910	0.418	−0.253	−0.735
480	2.062	0.434	−0.122	−0.741

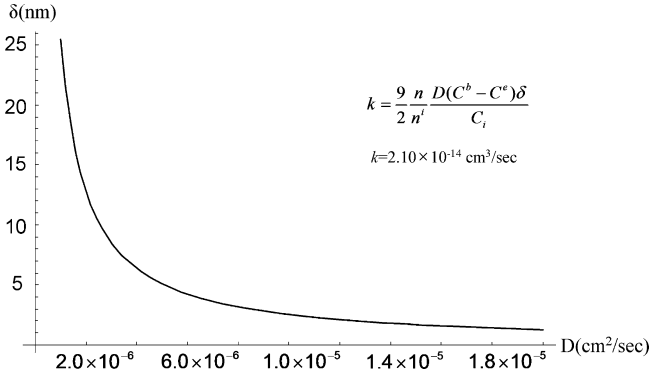

Fig. 7. Calculated relationship between diffusivity (D) of Cu through channel and channel width (δ).

solder into the grain boundaries of Cu_6Sn_5, and perhaps the exact width of the channel can be determined by transmission electron microscopy.

As the FDR assumes hemispherical scallops, it is of interest to see whether there is any change in ripening behavior when the scallop morphology deviates greatly from the hemispherical shape. Ghosh [10] investigated Ni_3Sn_4 formation by the reaction between various eutectic solders and Cu/Ni/Pd metallization. Ni_3Sn_4 scallops had an extremely faceted morphology, and their size distribution deviated greatly from the FDR theoretical curve. But their growth rate also followed $t^{1/3}$. Görlich et al. [11] investigated ripening of Cu_6Sn_5 when pure Sn reacted with Cu. The scallops had a faceted morphology, even though edges of scallops were more or less smoothened due to excessive chemical etching. The agreement with the theoretical model was not as good as in the current case of the round scallops, but was still in a relatively good agreement. The growth exponent was 0.34 for the scallop diameter and 0.40 for the height. This deviation from the theory can be examined in terms of geometric height-to-radius aspect ratio (height/(width/2)). In Görlich's work, average height-to-radius aspect ratio of scallops was ~0.71, while the average aspect ratio is 1.05 in the current study.

In the very early stage of the wetting reaction, nucleation of the scallops will have a greater effect on the size distribution. Thus, the PSD of short reaction time was expected to be less ideal. However, the size distribution of 30 s of reaction already showed very good agreement with the FDR theory. In addition, the standard deviations of PSD showed very little variation with reaction time (~0.4). This means that 30 s is enough time for ripening to be dominant over nucleation and growth and to achieve a stationary asymptotic state of distribution, which is stable in the reduced size scale $r/\langle r\rangle$.

5. Conclusion

In the wetting reaction between molten SnPb solder of varying composition and copper, the growth and ripening of Cu_6Sn_5 scallops obeys the FDR model of non-conservative ripening, assuming a constant interfacial area. The measured size distribution of the scallops is in good agreement with the FDR model, especially when the morphology of the scallops is close to hemispherical, as in the wetting reaction between eutectic SnPb and Cu. Minor deviations between the model and the experimental results can be reduced by taking noise into consideration, as is demonstrated in Appendix. The improved FDR model showed even better agreement with the experimental data.

Acknowledgement

The authors at UCLA would like to acknowledge the support from NSF contract DMR-0503726.

Appendix

The small difference between the measured statistical parameters and the theoretical values indicates that there is room for improvement of the FDR model. (This problem is also typical for PSD predicted by LSW theory for ripening in closed systems [12].) The origin of the deviation is considered to be from deviation of the local concentration of solute due to the large volume fraction of the scallops. The FDR theory was developed under mean field approximation, similar to the LSW theory. But if the new phase (precipitates or scallops) has a comparatively large volume fraction ($f > 0.02$) in standard Ostwald ripening, the deviations from the mean field caused by noise cannot be neglected [13]. The main origin of the noise is the deviation of local concentration (or chemical potential) from the mean field value in the parent phase. When a precipitate has a large volume fraction of closest neighbors, the closest neighbors will screen its diffusive interaction from more distant precipitates. Another reason for noise is the possible local fluctuations of diffusivity and surface tension. In the FDR theory, the volume fraction of scallops in the reaction zone is very large. The exact value of the volume fraction is difficult to tell. This is because the system is open near the scallops, and the scallops grow in the molten solder with a sharp concentration gradient in the scallop region. The copper atoms at the bottom of the scallops can be distributed only between the nearest neighboring scallops. In contrast, the copper atoms in the upper part of the solder bump can easily find their way to any scallop. It is assumed that the incoming Cu atoms have time and possibility to migrate all over the solder before attaching to some of the scallops. The volume fraction of scallops with average height h in the hemispherical solder bump with radius R can be roughly estimated as

$$f \approx \frac{\pi R^2 h}{\frac{2}{3}\pi R^3} \approx \frac{3}{2}\frac{h}{R} \tag{A1}$$

Even though this is a very rough estimation, the order of magnitude is correct. Take $h \approx 1.5\ \mu m$, which is about the average radius of scallops after 4 min reflow, and $R \approx 300\ \mu m$, which is about the radius of the solder bead. Then, one has $f \approx 0.0075$.

The noise level, the ratio of the average squared deviation of supersaturation in the vicinity of an arbitrary precipitate from the mean field value, is estimated as the equation below [13]:

$$v \equiv \frac{1}{\overline{\Delta}}\sqrt{\langle(\delta C)^2\rangle} \tag{A2}$$

where

$$\langle(\delta C)^2\rangle = \langle(\Delta - \overline{\Delta})^2\rangle \tag{A3}$$

where Δ is supersaturation in the vicinity of an arbitrary precipitate, and $\overline{\Delta}$ is the mean field value.

In a previous study [13], it was demonstrated that the noise level is approximately

$$v \approx f^{1/4} \cdot s \tag{A4}$$

where s is the standard deviation of PSD, which is equal to 0.215 in LSW and 0.33 in FDR. If one takes $s \approx 0.33$ and

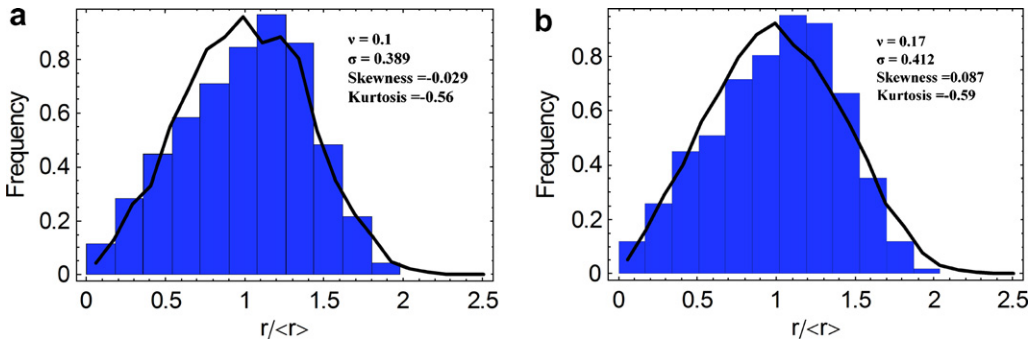

Fig. 8. Numerically calculated PSD (solid line) with noise of (a) $\nu = 0.1$ and (b) $\nu = 0.17$. Histogram in Fig. 6c is shown for comparison.

$f \approx 0.0075$ ($h \approx 1.5$ and $R \approx 300$ μm), $\nu \approx 0.1$. This can be considered as almost the lowest estimate of noise, because the short-range order effects and the possible scatter of channel widths were not considered. In the FDR model, the growth rate of the scallops is given as [4]

$$\frac{\mathrm{d}r_l}{\mathrm{d}t} = \frac{L}{nC_i}\left(\mu - \mu_\infty - \frac{\beta}{r_l}\right) \tag{A5}$$

where C_i is the quasi-equilibrium concentration of Cu in the vicinity of Cu_6Sn_5, μ is the average chemical potential of Cu in the reaction zone, μ_∞ is the equilibrium chemical potential for the flat interface, $\beta = 2\gamma\Omega$ (Ω is the molar volume, γ is the surface tension between the IMC and the liquid solder). The parameter L is similar to the Onsager coefficient and is determined self-consistently from the two constrains: constant surface and mass conservation [4].

Translating the noise of concentration into the noise of chemical potentials and adding the noise term, Eq. (A5) becomes

$$\frac{\mathrm{d}r_l}{\mathrm{d}t} = \frac{L}{n_i C_i}\left((\mu - \mu_\infty)\cdot(1+\varepsilon_l) - \frac{\beta}{r_l}\right) \tag{A6}$$

where ε_l is the relative noise of the chemical potential and the corresponding copper concentration, in the vicinity of the lth scallop. The ε_l is taken to be distributed according to Gaussian distribution with standard deviation, determined by the noise level ν.

As the total surface area of the particles is assumed to be constant in the FDR theory, one must substitute Eq. (A6) into the constraint of constant total surface $\mathrm{d}S/\mathrm{d}t = 0$

$$\begin{aligned}\frac{\mathrm{d}S}{\mathrm{d}t} &= 2\sum_l 2\pi r_l \frac{\mathrm{d}r_l}{\mathrm{d}t} \\ &= \frac{4\pi L}{n_i C_i}\left(\sum_l (\mu-\mu_\infty)(1+\varepsilon_l)r_l - N\beta\right) = 0\end{aligned} \tag{A7}$$

which gives

$$\mu - \mu_\infty = \frac{\beta}{\langle r\rangle + \langle \varepsilon r\rangle} \tag{A8}$$

In the FDR theory, it was assumed that all the incoming flux of copper is consumed by the growth in the total volume of the scallops. As a result, it was shown that [4]

$$\frac{3}{2}\frac{n}{n_i}\delta\frac{D\Delta C}{C_i} = \frac{3}{N}\sum_l r_l^2\frac{\mathrm{d}r_l}{\mathrm{d}t} \tag{A9}$$

Applying Eqs. (A6) and (A8) to (A9)

$$\begin{aligned}\frac{1}{2}\frac{n}{n_i}\delta\frac{D\Delta C}{C_i} &= \frac{1}{N}\sum_l r_l^2\frac{\mathrm{d}r_l}{\mathrm{d}t} \\ &= \frac{L}{n_i C_i N}\sum_l r_l^2\left(\frac{\beta(1+\varepsilon_l)}{\langle r\rangle + \langle \varepsilon r\rangle} - \frac{\beta}{r_l}\right) \\ &= \frac{L\beta}{n_i C_i}\left(\frac{\langle r^2\rangle + \langle \varepsilon r^2\rangle}{\langle r\rangle + \langle \varepsilon r\rangle} - \langle r\rangle\right) \\ &= \frac{L\beta}{n_i C_i}\frac{\langle r^2\rangle - \langle r\rangle^2 + \langle \varepsilon r^2\rangle - \langle r\rangle\langle \varepsilon r\rangle}{\langle r\rangle + \langle \varepsilon r\rangle}\end{aligned} \tag{A10}$$

Eq. (A10) immediately gives, together with Eqs. (A6) and (A8)

$$\frac{\mathrm{d}r_l}{\mathrm{d}t} = \frac{k}{9}\frac{(1+\varepsilon_l) - \frac{\langle r\rangle + \langle \varepsilon r\rangle}{r_l}}{\langle r^2\rangle - \langle r\rangle^2 + \langle r^2\varepsilon\rangle - \langle r\rangle\langle r\varepsilon\rangle} \tag{A11}$$

with

$$k = \frac{9}{2}\frac{n}{n_i}\frac{D\Delta C}{C_i}\delta \tag{A12}$$

So far, one can only treat this problem numerically.

A simple numerical method developed for LSW case was used for noise in the FDR case [13]. Taking into account that scallops are consumed one by one by their more successful competitors, one can numerically solve the set of N differential equations for squared radii

$$\frac{\mathrm{d}r_l^2}{\mathrm{d}t} = \frac{2k}{9}\frac{r_l(1+\varepsilon_l) - \langle r\rangle - \langle \varepsilon r\rangle}{\langle r^2\rangle - \langle r\rangle^2 + \langle r^2\varepsilon\rangle - \langle r\rangle\langle r\varepsilon\rangle} \tag{A13}$$

Fig. 8 presents size distributions for different noise levels obtained by the numerical method. The histogram in Fig. 6c is shown along with numerically calculated curves for comparison. The noise leads to broader, more symmetrical and less sharp distributions. The distribution should change with time owing to the noise, but the standard deviation tends to converge to some limit, depending on the noise level. If one takes $\nu = 0.1$, the standard deviation, skewness and kurtosis are 0.389, −0.029 and −0.56, respectively. If $\nu = 0.17$, they are 0.412, 0.087 and −0.59, which is closer to the experimental data.

References

[1] Kim HK, Tu KN. Phys Rev B 1996;53:16027–34.
[2] Lifshitz IM, Slyozov VV. J Phys Chem Solids 1961;19:35–50.
[3] Wagner CZ. Elektrochem 1961;65:581–91.
[4] Gusak AM, Tu KN. Phys Rev B 2002;66(11):115403.
[5] Tu KN, Gusak AM, Li M. J Appl Phys 2003;93(3):1335–53.
[6] ASM. Metals handbook, 9th ed., vol. 9. Materials Park, OH: ASM; 1985. p. 416.
[7] Jackson KA. Prog Solid State Chem 1967;4:53–80.
[8] Temkin DE. Molecular roughness of the crystal-melt boundary. In: Sirota NN, Gorskii FK, Varikash VM, editors. Crystallization processes. New York (NY): Consultants Bureau; 1966. p. 15–23.
[9] Liu CY, Tu KN. J Mater Res 1998;13:37–44.
[10] Ghosh G. J Appl Phys 2000;88:6887–96.
[11] Görlich J, Schmitz G, Tu KN. Appl Phys Lett 2005;86:053106.
[12] Ardell AJ. Precipitate coarsening in solids: modern theories, chronic disagreement with experiment. In: Lorimer GW, editor. Phase transformations'87. London: Institute of Metals; 1988. p. 485–94.
[13] Gusak AM, Lutsenko GV. Philos Mag 2005;85:1323–31.